Analysis of lunar pyroclastic deposit FeO abundances by LRO Diviner

Carlton C. Allen,[1] Benjamin T. Greenhagen,[2] Kerri L. Donaldson Hanna,[3] and David A. Paige[4]

Received 30 September 2011; revised 25 May 2012; accepted 4 June 2012; published 21 August 2012.

[1] Thermal infrared reflectance spectra of rock-forming minerals include a prominent minimum near 8 μm, known as the "Christiansen feature" (CF). The inflection point wavelength is sensitive to the degree of polymerization of silicates, which is strongly influenced by major cations – notably iron – in the minerals. Laboratory spectra of lunar soils demonstrate that the CF location is closely correlated to the sample's bulk FeO abundance, across the full range of Apollo soil samples, including pyroclastic glass. This correlation is the basis for estimating lunar surface FeO abundances using orbital thermal infrared measurements. The Diviner Lunar Radiometer Experiment on the Lunar Reconnaissance Orbiter includes three thermal infrared channels, selected to determine the CF positions for sites across the lunar surface. Diviner measurements are used to derive FeO abundances in the Aristarchus, Sulpicius Gallus, and Rima Fresnel pyroclastic deposits. The calculated FeO abundances for Aristarchus and Sulpicius Gallus lie within the compositional range of FeO-rich pyroclastic glasses but outside the range of most mare soils, supporting the interpretations of these deposits as glass rich. The calculated FeO abundance for the Rima Fresnel deposit is close to that of mare soils, supporting a contention that this deposit is dominated by basaltic fragments rather than glass. The Diviner measurements hold the potential to determine FeO abundances in many lunar pyroclastic deposits. A better understanding of these compositions will provide insight into the magmatic history and composition of the lunar interior, as well as an enhanced inventory of potential resources for future human exploration.

Citation: Allen, C. C., B. T. Greenhagen, K. L. Donaldson Hanna, and D. A. Paige (2012), Analysis of lunar pyroclastic deposit FeO abundances by LRO Diviner, *J. Geophys. Res.*, *117*, E00H28, doi:10.1029/2011JE003982.

1. Background

[2] The objective of this investigation is to assess the relationship between the thermal infrared spectra and FeO abundances of lunar soils and pyroclastic glasses. Laboratory measurements of well-characterized Apollo samples provide the basis for interpreting spectroscopic data from the Diviner Lunar Radiometer Experiment on the Lunar Reconnaissance Orbiter (LRO).

[3] *Lunar Pyroclastic Deposits.* Telescopic observations and orbital images of the Moon reveal at least 75 low-albedo deposits, many of them tens to hundreds of kilometers across, which partially mantle mare or highland surfaces [*Gaddis et al.*, 2003]. These deposits are interpreted as the products of pyroclastic eruptions [*Head*, 1974], and are designated herein as lunar pyroclastic deposits (LPD). The eruption products of the various deposits are interpreted to include beads of pyroclastic glass with differing degrees of crystallinity, as well as finely fractured basalt [*Gaddis et al.*, 2003].

[4] The Taurus Littrow LPD (Figure 1), located in eastern Mare Serenitatis, covers an area of 2,940 km^2 [*Gaddis et al.*, 2003] and is approximately ten meters thick [*Heiken et al.*, 1974]. Material from this LPD extends across the Apollo 17 landing site. Black and orange glass beads from surface exposures and drill cores collected by the Apollo 17 astronauts (Figure 2) have long been understood to be samples of the Taurus Littrow LPD [*Pieters et al.*, 1974; *McKay et al.*, 1978]. The orange and black beads are identical in elemental composition, with the black beads being largely crystalline and the orange beads largely vitreous. This difference has been interpreted to reflect cooling dynamics in the eruption cloud [*Weitz et al.*, 1999]. Apollo 17 drill core sample 74002, discussed below, contains over 90 modal percent black and orange beads [*McKay et al.*, 1978].

[5] *Delano* [1986] documented 25 distinct pyroclastic bead compositions in lunar soil samples from the Apollo

[1]NASA Johnson Space Center, Houston, Texas, USA.
[2]Jet Propulsion Laboratory, Pasadena, California, USA.
[3]Department of Geological Sciences, Brown University, Providence, Rhode Island, USA.
[4]Department of Earth and Space Sciences, University of California, Los Angeles, California, USA.

Corresponding author: C. Allen, NASA Johnson Space Center, Mail Code KT, Houston, TX 77058, USA. (carlton.c.allen@nasa.gov)

©2012. American Geophysical Union. All Rights Reserved.
0148-0227/12/2011JE003982

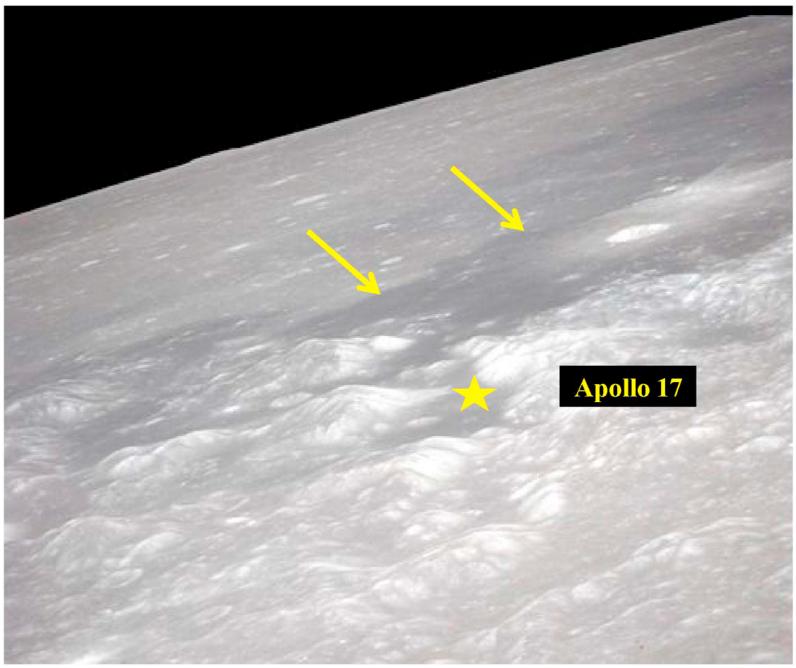


Figure 1. Taurus Littrow pyroclastic deposit (arrows) in eastern Mare Serenitatis; star shows location of the Apollo 17 landing site; (NASA image AS17-148-22770).

sites. Glass colors include green, yellow, orange, and red and are generally correlated with each sample's titanium abundance. Iron, calculated as FeO, abundances in the glass beads reported by *Delano* [1986] range from 16.5–24.7 wt%. Titanium, calculated as TiO_2, ranges from 0.26–16.4 wt. %. Many of these compositions are represented by individual beads sparsely dispersed in lunar soil samples. A few Apollo samples, however, consist almost entirely of such beads, including Apollo 17 orange and black glass (Figure 2) and Apollo 15 green glass. With the exception of the Taurus Littrow LPD, the source deposits of these pyroclastic glasses have not been identified.

[6] Several of the larger pyroclastic deposits have been extensively studied, and their visible and near-infrared spectra have been used to estimate glass concentrations and major element abundances [*Hawke et al.*, 1989; *Weitz et al.*, 1998; *Blewett and Hawke*, 2001; *Wilcox et al.*, 2006]. Orbital thermal infrared measurements have the potential to provide an independent tool to derive FeO abundance, a useful indicator of pyroclastic deposit compositions across the entire lunar surface.

[7] The pyroclastic deposits are important for a variety of reasons. Petrology experiments and modeling have demonstrated that pyroclastic glasses represent the deepest-sourced and most primitive magmas on the Moon [*Green et al.*, 1975]. Recent analyses have documented the presence of water in these glasses, demonstrating that the lunar interior is considerably more volatile-rich than previously understood [*Saal et al.*, 2008]. High-temperature hydrogen reduction experiments have shown that the FeO-rich pyroclastic glasses release the highest percentage of oxygen of any Apollo soils [*Allen et al.*, 1996], making these deposits promising lunar resources. The combination of scientific interest and resource potential has kept pyroclastic deposits among the

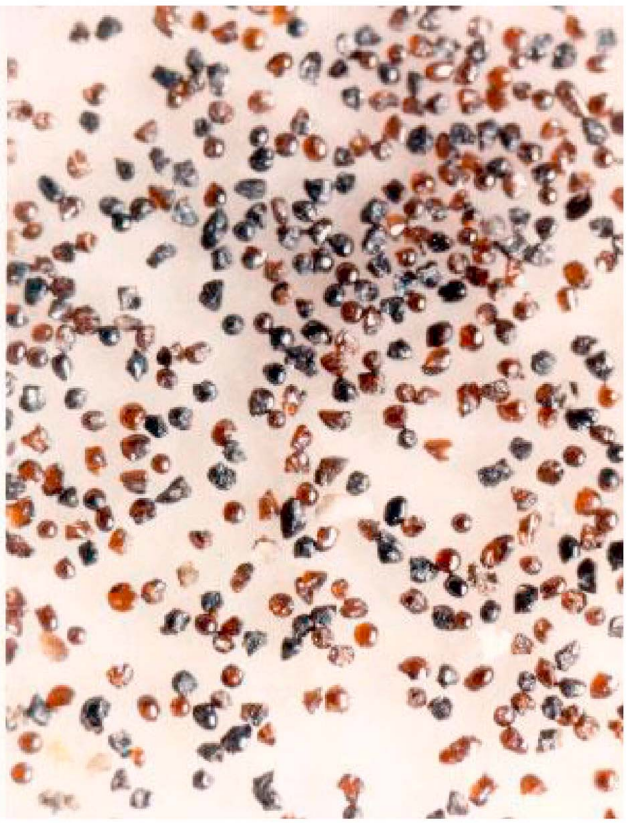


Figure 2. Sieved and washed fraction of surface sample 74220, consisting almost exclusively of black and orange glass beads; typical particle size is approximately 100 μm (NASA image S73–15085).

Table 1. I_s/FeO (Maturity), CF Values (μm) Derived From RELAB Spectra, Published FeO and TiO_2 Abundances (wt. %) for 5 Lunar Soils (20–45 μm Size Fractions) As Well As Pyroclastic Glasses 74002 and 15401 (Bulk Samples)

Apollo	Sample	I_s/FeO	CF	FeO	TiO_2
11	10084	67	8.39	15.5	8.30
12	12001	51	8.35	16.9	3.20
15	15041	66	8.31	15.2	2.03
16	61141	76	8.19	5.2	0.58
17	70181	53	8.42	16.0	8.11
17	74002	<1	8.63	22.7	9.2
15	15401	6	8.39	16.3	1.08

best-studied prospects for a future lunar base [*Coombs et al.*, 1998].

[8] *Measuring FeO from Lunar Orbit.* The use of Diviner thermal infrared spectrometry, described below, is the most recent effort to calculate lunar FeO abundances from orbital data. Ultraviolet- visible - and near-infrared data from the Clementine spacecraft, along with gamma-ray and neutron data from Lunar Prospector, have been used by multiple authors to derive increasingly refined estimates of FeO abundances [*Lucey et al.*, 1995; *Blewett et al.*, 1997; *Lucey et al.*, 1998, 2000; *Lawrence et al.*, 2002; *Le Mouélic et al.*, 2002; *Wilcox et al.*, 2005]. *Blewett and Hawke* [2001] and *Wilcox et al.* [2006] calculated FeO abundances for the Aristarchus, Sulpicius Gallus, and Rima Fresnel pyroclastic deposits, which were analyzed using Diviner data in the current investigation.

2. Laboratory Measurements

[9] *Christiansen Feature.* Thermal infrared reflectance spectra of rock-forming minerals include a prominent reflectance minimum centered near 8 μm, known as the "Christiansen feature" (CF). The inflection point wavelength is sensitive to the degree of polymerization of silicate minerals [*Logan et al.*, 1973; *Salisbury et al.*, 1973], and the major minerals of lunar soils – plagioclase, pyroxene, and olivine – each have distinctly different ranges of CF values. Lunar soils also contain significant fractions of agglutinic glass, with CF wavelengths in the same locations as their corresponding crystalline materials [*Nash*, 1991]. Laboratory studies have demonstrated that thermal infrared laboratory spectra of lunar soil samples clearly discriminate between soils dominated by highland or mare components [*Logan et al.*, 1975].

[10] The CF value for a lunar soil is strongly correlated to the soil's proportions of plagioclase, pyroxene, and olivine and thus by inference to the major element compositions of these minerals. This simplicity of soil compositions leads specifically to the hypothesis that CF values for lunar soils may be correlated with the samples' bulk FeO abundances.

[11] *Lunar Soils.* This hypothesis was tested using data from Apollo soil samples characterized in detail by the Lunar Soil Characterization Consortium (LSCC) [*Taylor et al.*, 2001, 2010]. To determine major element concentrations, sieved subsamples of pristine soils were prepared as fused glass beads and analyzed by electron microprobe (Tables 1 and 2). Spectral reflectance measurements of sieved subsamples from these soils were obtained under ambient conditions using a Nicolet 870 Nexus FT-IR spectrometer in the Keck/NASA Reflectance Experiment Laboratory (RELAB) at Brown University [*Pieters and Hiroi*, 2004]. The spectrum of each sample included a well-defined reflectance minimum in the vicinity of 8 μm (Figure 3). The wavelength corresponding to the minimum reflectance value in each data set was taken as the CF wavelength. The spectral resolution of RELAB data near 8 μm is 0.01 μm.

[12] The LSCC [*Taylor et al.*, 2001, 2010] focused on the <45 μm fractions of lunar soils, the size fraction understood to dominate the spectral properties of bulk soil [*Pieters et al.*, 1993]. The present study employed data from the 20–45 μm sieve fractions of the soil samples, considered to be the size fraction most strongly controlling the thermal infrared spectra (L. A. Taylor, personal communication, 2009).

[13] CF values from RELAB spectra were determined for 5 lunar soil samples, including one sample each from Apollo missions 11, 12, 15, 16, and 17. These soils span essentially the entire compositional range in the Apollo collection. The samples were part of a larger set of soils characterized by the LSCC and having reflectance spectra in the RELAB data set. The five specific samples chosen for this study each has a maturity index (I_s/FeO) between 51 and 76 [*Morris*, 1978]. This selection was made to minimize the effects of maturity on CF values, discussed below. No Apollo 14 sample was found that met all of these criteria, but the FeO abundances of the soils that were included span the abundances of Apollo 14 samples.

[14] *Pyroclastic Glasses.* RELAB measurements have also been made of Apollo 17 orange and black glass beads and Apollo 15 green glass beads, the only samples of pyroclastic glass large enough for such measurements. Five separate subsamples of lunar sample 74002, a portion of an Apollo 17 drill core dominated by orange and black beads, were measured. The subsamples were taken from depths ranging from 1 mm to 24 cm below the surface. Based on the point counting studies of *Nagle* [1978], the ratio of orange:black beads among these five subsamples ranges from approximately 70:30 to 20:80. While these are bulk samples, the beads are mainly smaller than 100 μm in diameter, with an average grain size along the entire core of 40 +/− 5 μm [*McKay et al.*, 1978]. The mean RELAB CF value for these five subsamples is 8.63 μm (standard deviation = 0.02 μm). *Weitz et al.* [1999] conducted microprobe analyses of multiple orange glass beads from thin sections of sample 74220, and reported that most compositions cluster around FeO concentrations of 22.7 +/− 0.2 wt. % and TiO_2 concentrations of 9.2 +/− 0.2 wt. %.

Table 2. Mean CF Values (μm) for 2 × 2 km Areas Near Apollo Landing Sites and Taurus Littrow LPD (TAUL), Derived From Diviner Measurements[a]

Apollo	CF	Std Dev	Sample	FeO
11	8.29	0.04	10084	15.5
12	8.28	0.01	12001	16.9
15	8.30	0.03	15041	15.2
16	8.15	0.01	61141	5.2
17	8.33	0.03	70181	16.0
TAUL	8.36	0.03	74002	22.7

[a]Standard deviations (μm) determined from data values; published FeO abundances (wt. %) of 20–45 μm size fractions of 5 lunar soils as well as pyroclastic glass 74002 (bulk sample).

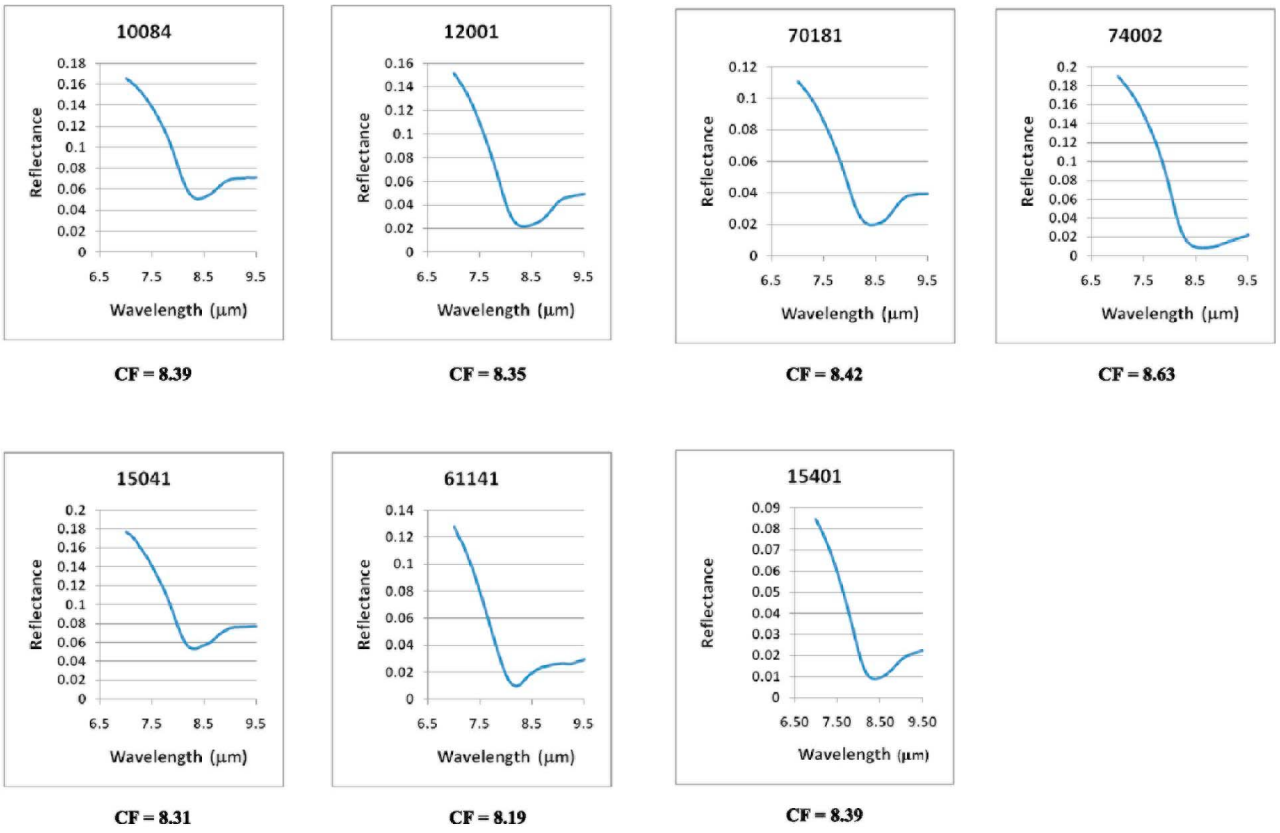


Figure 3. RELAB reflectance spectrum of 5 Apollo soils (20–45 μm sieve fraction) as well as pyroclastic glasses 74002 and 15401 (bulk samples); CF value (μm) equals the reflectance minimum for each sample; RELAB spectral resolution = 0.01 μm.

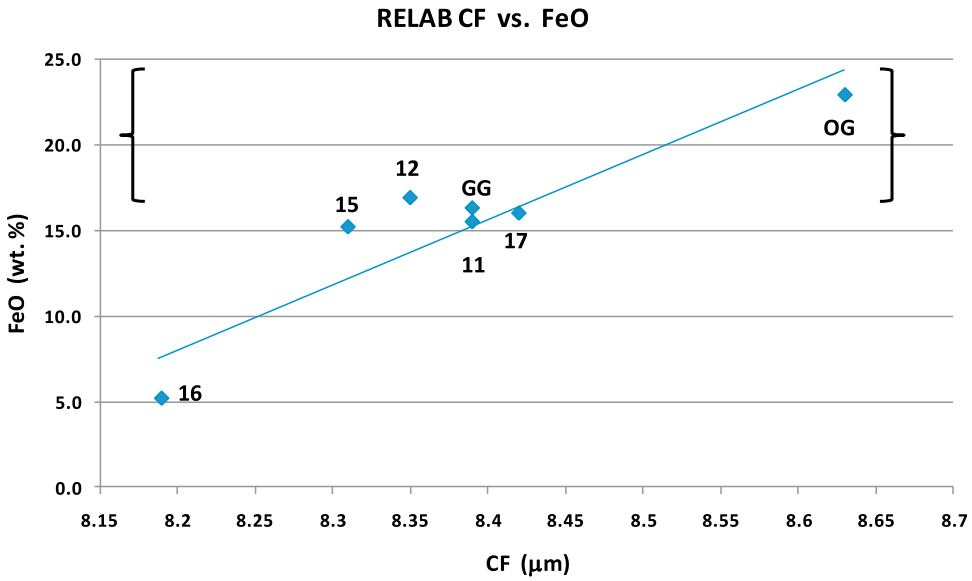


Figure 4. Correlation of RELAB CF wavelengths with published FeO abundances for 5 lunar soils (20–45 μm sieve fractions) as well as pyroclastic glasses 74002 and 15401 (bulk samples); data in Table 1; soil samples identified by Apollo mission; GG = green glass 15401; OG = orange/black glass 74002; brackets denote range of pyroclastic glass FeO abundances [*Delano*, 1986]; regression line: FeO = 35.48 × CF − 282.0; r^2 = 0.83.

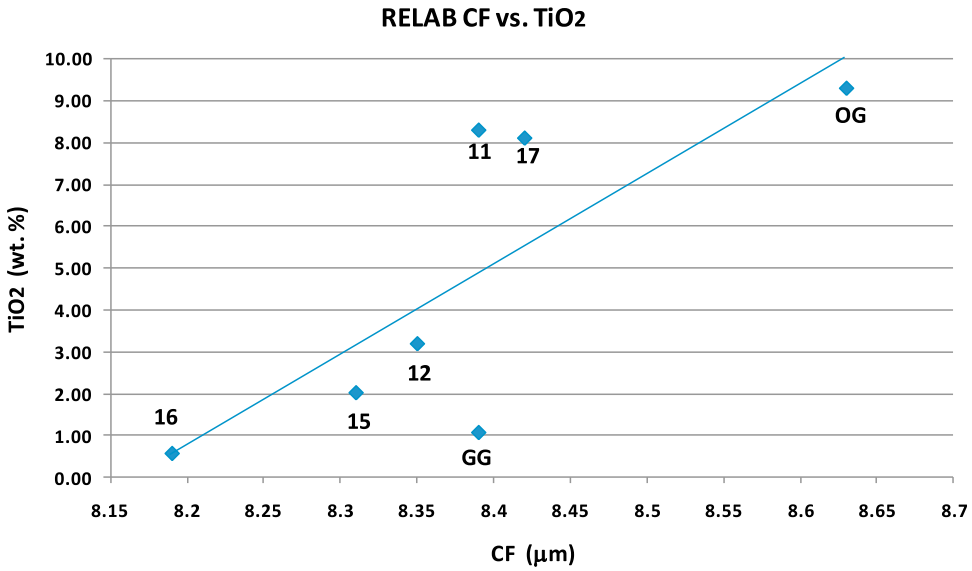


Figure 5. Correlation of RELAB CF wavelengths with published TiO_2 abundances for 5 lunar soils (20–45 μm sieve fractions) as well as pyroclastic glasses 74002 and 15401 (bulk samples); data in Table 1; soil samples identified by Apollo mission; GG = green glass 15401; OG = orange/black glass 74002; regression line: $TiO_2 = 21.45 \times CF - 175.19$; $r^2 = 0.58$.

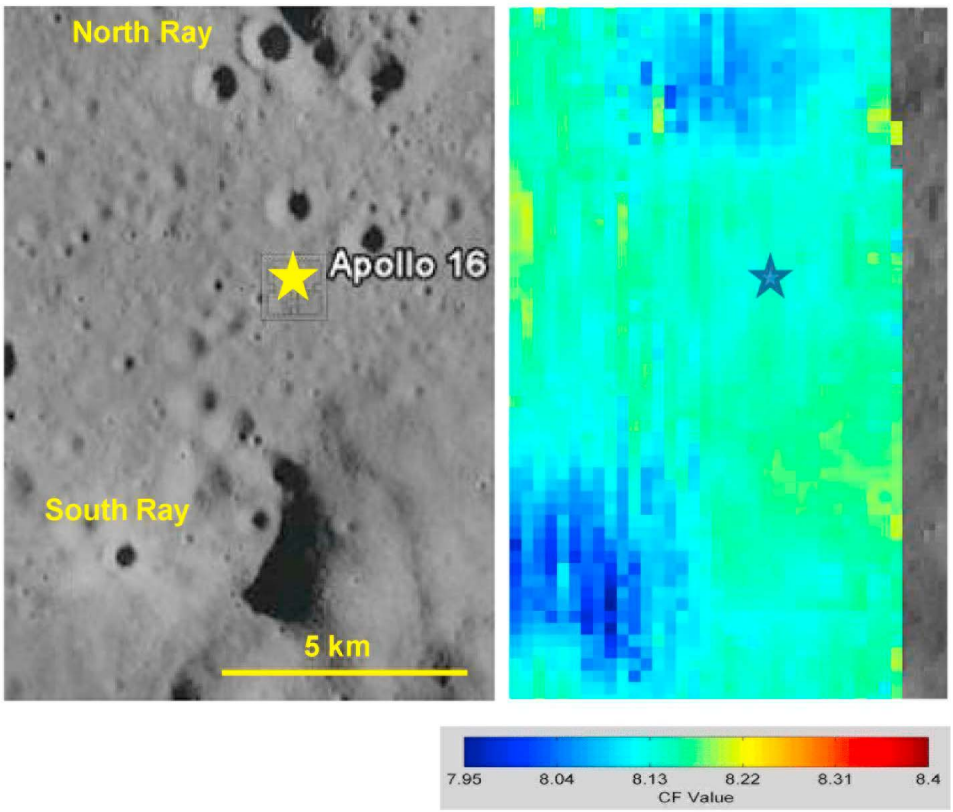


Figure 6. Apollo metric camera image of the Apollo 16 landing site vicinity (left), and corresponding Diviner CF false-color image (right) covering the same area and orientation; colors correspond to corrected CF values; stars shows location of the landing site; low-CF areas north and south of the landing site map the ejecta of North Ray and South Ray craters; corrected CF in 2 × 2 km area near landing site = 8.15 +/− 0.01 μm (NASA image AS16-M-0440).

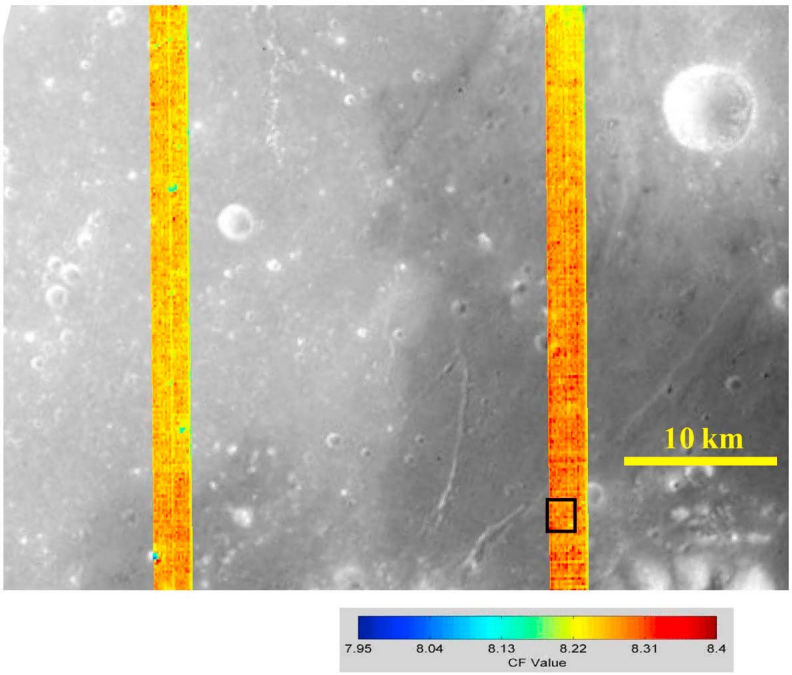


Figure 7. Taurus Littrow pyroclastic deposit and eastern Mare Serenitatis with Diviner data strips from consecutive orbits color coded by CF over Apollo 15 metric camera image; 2 × 2 km area selected to determine mean CF value (20°45′N, 29°21′E) denoted by black box at lower right; corrected CF = 8.36 +/− 0.03 μm (NASA image AS15-M-1403).

[15] Apollo 15 soil 15401 contains a large proportion of green glass beads. The average grain size of this soil is 89 μm [*Graf*, 1993]. The RELAB CF value for a bulk sample of 15041 is 8.39 μm. The published FeO abundance is 16.3 wt. % and its TiO_2 abundance is 1.08 wt. %, determined by instrumental neutron activation analysis [*Korotev*, 1987].

[16] *FeO Abundance.* Figure 4 is a plot of CF values derived from RELAB spectra correlated with published FeO abundances for these 5 lunar soils and 2 pyroclastic glass samples. The plot demonstrates the general linear correlation between CF and FeO over almost the entire range of FeO concentrations represented in the Apollo collection, from approximately 5–23 wt. %.

[17] The slope of the correlation line is 35.48. The goodness of fit for this linear correlation, as expressed by the r^2 value, is 0.83. The two pyroclastic glass compositions fall on or near the linear trend.

[18] *TiO_2 Abundance.* Figure 5 shows the correlation between CF and TiO_2 for the same 5 lunar soils and 2 pyroclastic glass samples. The plot shows a roughly linear trend with much more scatter than the trend for CF correlated with FeO (Figure 4), as indicated by an r^2 value of 0.58 for the titanium plot. The point corresponding to the Apollo 15 green glass sample falls well off the regression line. This comparison demonstrates that CF is much more closely correlated with lunar soil and pyroclastic glass FeO abundance than with TiO_2 abundance. The analyses below, therefore, are confined to FeO abundance.

3. Orbital Measurements

[19] The sensitivity of CF wavelength to lunar soil mineralogy was demonstrated shortly after the Apollo samples were collected [*Salisbury et al.*, 1973], and the potential of this relationship for lunar remote sensing was immediately appreciated [*Logan et al.*, 1973, 1975]. This potential is now being realized, with CF values for the entire Moon being derived from data obtained in lunar orbit [*Greenhagen et al.*, 2010].

[20] *Diviner.* The Diviner Lunar Radiometer Experiment is a near- and thermal infrared mapping radiometer with nine 21-element arrays of uncooled thermopile detectors [*Paige et al.*, 2009]. Diviner has been mapping from a polar orbit in monthly cycles since shortly after LRO reached the Moon in June, 2009. The spacecraft altitude has been changed several times during the mission, but most of the observations reported here were obtained from an altitude of approximately 50 km. At this altitude Diviner has a 320 m (in track) by 160 m (cross track) detector field of view and a 3.4 km swath width.

[21] Diviner includes three detectors with filters that span the wavelength ranges 7.55–8.05 μm, 8.10–8.40 μm, and 8.38–8.68 μm. These "8 μm-region channels" were specifically selected to allow determination of the CF position as an emissivity maximum [*Greenhagen et al.*, 2010]. The precision of individual Diviner CF values is estimated at <0.02 μm. These CF values are known to be systematically affected by illumination and viewing geometry, and the data used in the analyses described below were restricted to a range where these effects are minimized. All data used in the current study were reduced using the most recent corrections of *Greenhagen et al.* [2011].

[22] *Apollo Landing Sites.* Diviner CF data demonstrate the compositional variability of lunar soil at the 100 m scale, as well as the contribution of impact craters that penetrate the soil and eject substrate materials of different compositions or

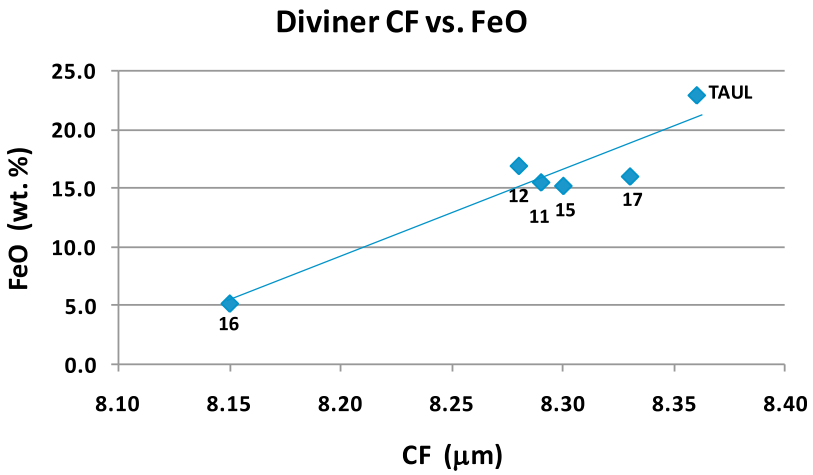


Figure 8. Correlation of Diviner CF values with sample FeO concentrations for 5 Apollo sites plus the Taurus Littrow pyroclastic deposit; CF values and standard deviations in Table 2; regression line: FeO = 74.24 × CF − 599.9; r^2 = 0.90.

maturity. Figure 6 illustrates the generally homogeneous soil composition near the Apollo 16 landing site, along with the fresh, spectrally distinct ejecta of North Ray and South Ray craters.

[23] Diviner CF values were derived for 2 × 2 km areas centered near the Apollo 11, 12, 15, 16, and 17 landing sites. All data were taken near lunar mid-day to maintain consistent lighting and soil temperatures. The mean CF value for each 2 × 2 km block was determined, along with the standard deviation attributable to counting statistics and local soil heterogeneity. These standard deviation values range from 0.01–0.04 μm for the locations measured (Table 2). The

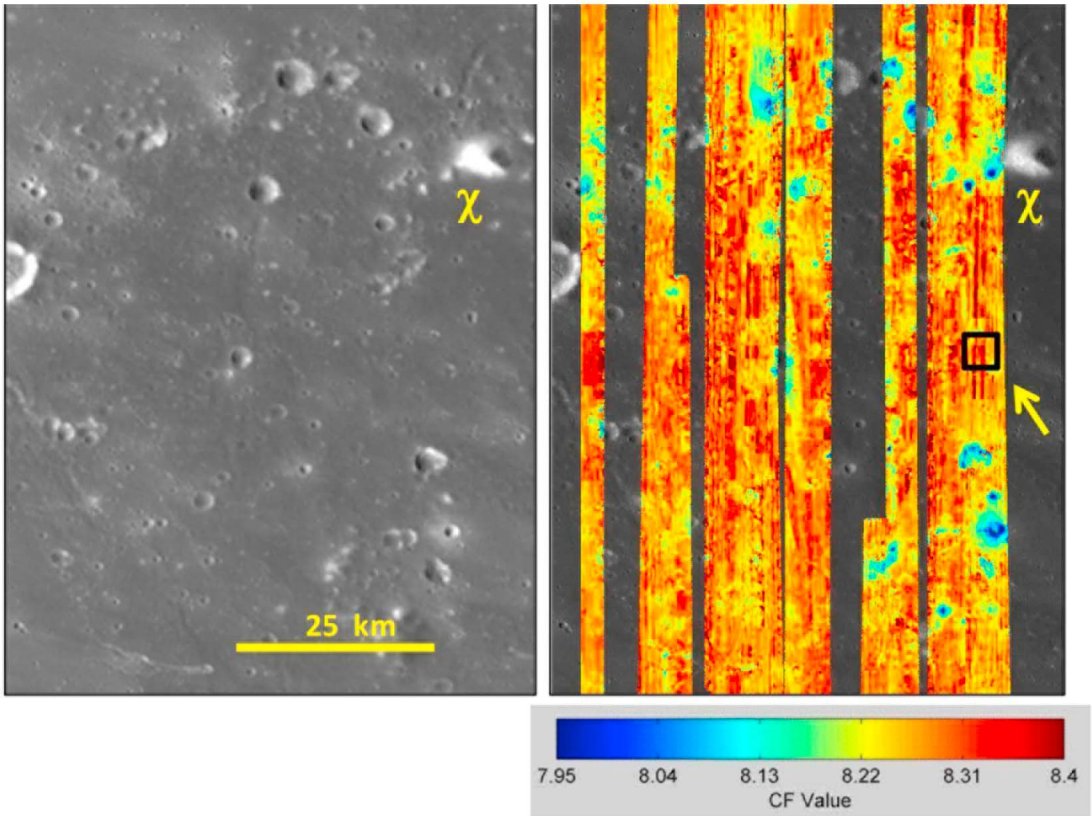


Figure 9. Aristarchus – LRO Wide-angle Camera mosaic (see http://wms.lroc.asu.edu/lroc/global_product/100_mpp_global_bw) and Diviner CF values covering the same area and orientation; Herodotus χ location marked; 2 × 2 km block for CF derivation (26°51′N, 52°22′W) denoted by black box and arrow; corrected CF = 8.34 +/− 0.03 μm.

Table 3. Calculated FeO Abundances and Standard Deviations (wt. %) for Four Sites at Three Lunar Pyroclastic Deposits

Lunar Pyroclastic Deposit	FeO	Std Dev
Aristarchus	19.3	2.2
Sulpicius Gallus	21.6	3.0
Rima Fresnel	17.8	3.0
Rima Fresnel	15.6	2.2

mean CF values were correlated (Table 2) to published FeO abundances for the 20–45 μm sieve fractions of the same Apollo soil samples used in the RELAB study discussed above [*Taylor et al.*, 2001, 2010].

[24] *Taurus Littrow.* Diviner CF values were also derived for an area in the Taurus Littrow LPD, near 20°45′N, 29°21′E (Figure 7). This location was chosen to represent minimally contaminated pyroclastic material, with CF values typical of the deposit and a low degree of CF variation. Corrected CF values were averaged over a 2 × 2 km area. The mean CF wavelength is 8.36 μm, with a standard deviation of 0.03 μm. This value, plotted against a FeO concentration of 22.7 wt% derived from pyroclastic glass sample 74002, lies close to the linear trend between Diviner CF measurements and lunar soil FeO abundances (Figure 8). Incorporating this value provides a regression that spans nearly the entire compositional range of granular materials in the Apollo collection. The slope of this regression line is 74.24 and the goodness of fit (r^2) value is 0.90.

4. Diviner Measurements of CF for Lunar Pyroclastic Deposits

[25] The correlation between Diviner CF and sample FeO provides a basis for remote analysis of the FeO concentrations in lunar pyroclastic deposits other than Taurus Littrow. Three such deposits with different sizes and geologic settings – Aristarchus, Sulpicius Gallus, and Rima Fresnel – have been investigated.

[26] *Aristarchus.* This pyroclastic deposit spans most of the Aristarchus plateau, a highlands crustal block measuring approximately 170 km by 200 km that rises over 2 km above Oceanus Procellarum. This is the largest LPD identified, with an area of 49,013 km^2 [*Gaddis et al.*, 2003]. The deposit displays a range of pyroclastic glass concentrations and spectral signatures, possibly from mixing with underlying material due to cratering. *Wilcox et al.* [2006], using radiative transfer modeling, estimated a FeO concentration for the Aristarchus pyroclastic deposit of 20.75 wt. %.

[27] *Weitz et al.* [1998] mapped seven major LPDs using Clementine ultraviolet and visible data, and determined that the Aristarchus plateau material had the reddest color and the strongest glass band absorption of any of these deposits. They estimated that the pyroclastic deposit in many places was mixed with highland or mare material, and that one of

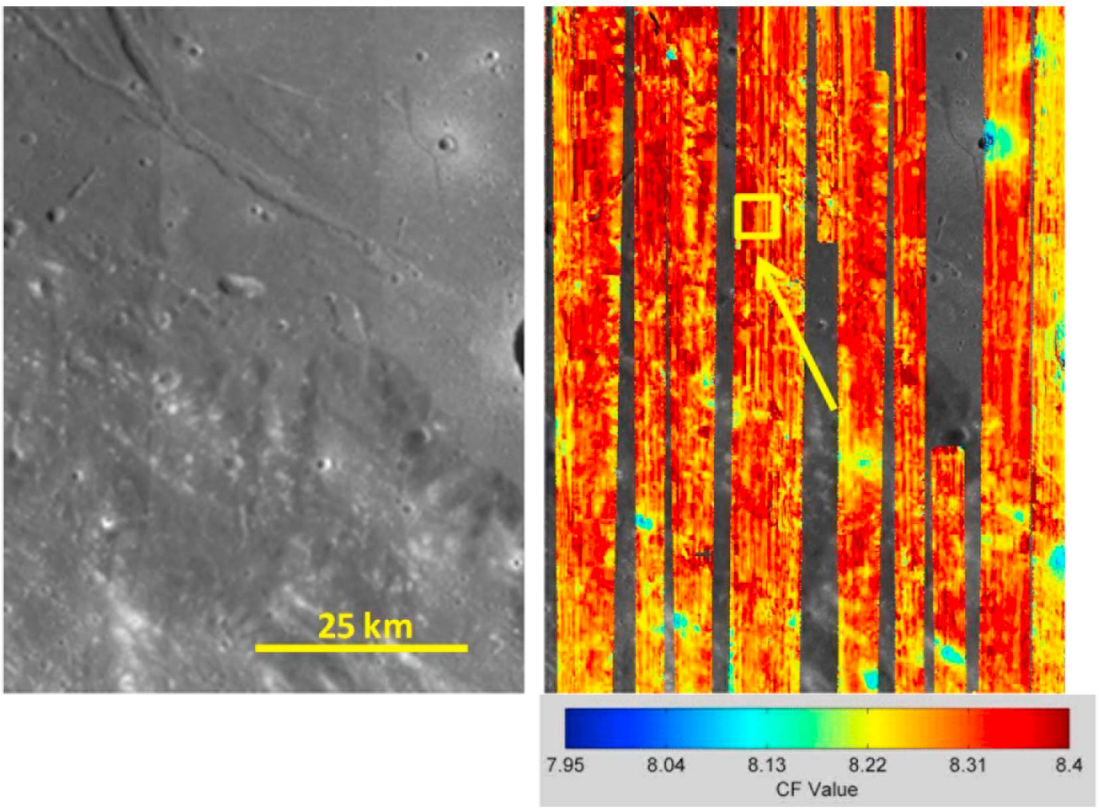


Figure 10. Sulpicius Gallus – LRO Wide-angle Camera mosaic (see http://wms.lroc.asu.edu/lroc/global_product/100_mpp_global_bw) and Diviner data strips color coded to CF values; 2 × 2 km block for CF derivation (20°9′N, 10°17′E) denoted by yellow box and arrow; corrected CF = 8.37 +/− 0.04 μm.

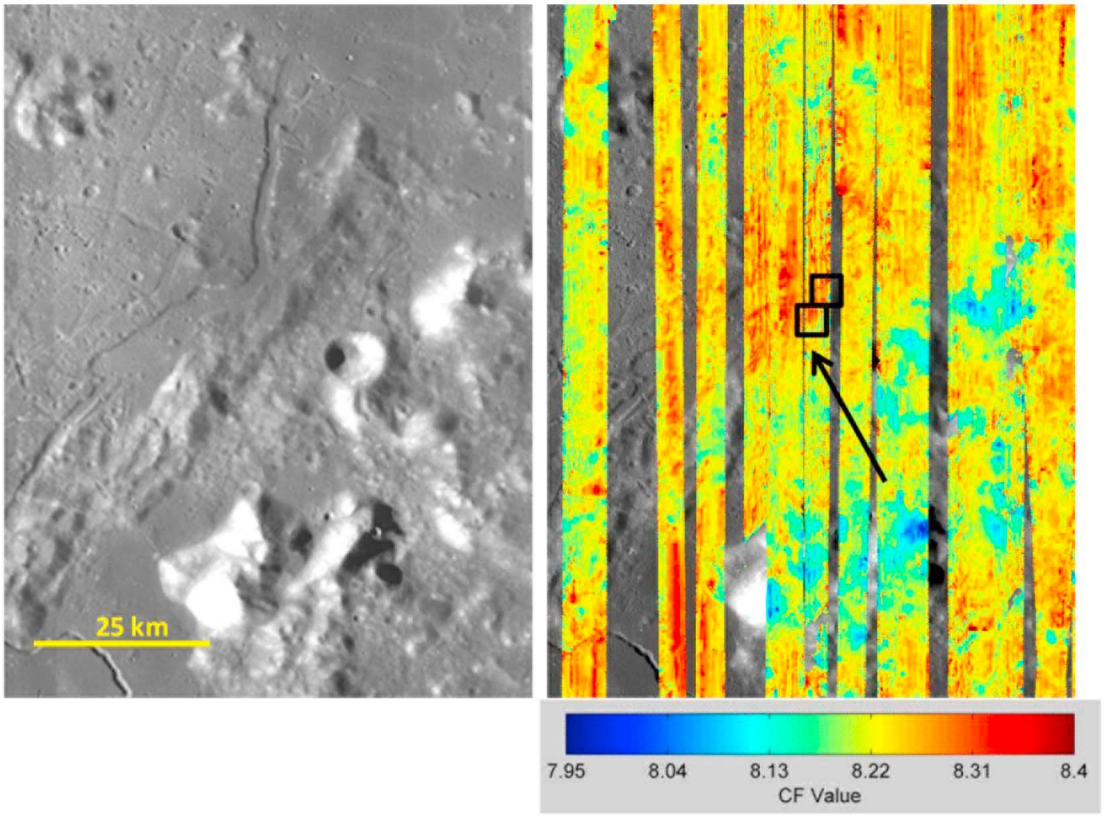


Figure 11. Rima Fresnel – LRO Wide-angle Camera mosaic (see http://wms.lroc.asu.edu/lroc/global_product/100_mpp_global_bw) and Diviner CF values covering the same area and orientation; two closely spaced 2 × 2 km areas for CF derivation (28°3′N, 4°18′E) denoted by black boxes and arrow; corrected CF (upper block) = 8.32 +/− 0.04 μm; corrected CF (lower block) = 8.29 +/− 0.03μm.

the highest concentrations of pyroclastic glass was located near Herodotus χ, a bright hill in the northwest region of the plateau.

[28] The mean CF value for a 2 × 2 km area near 26°51′N, 52°22′W, in the vicinity of Herodotus χ, is 8.34 μm, with a standard deviation of 0.03 μm (Figure 9). The regression line formula (Figure 8) translates the Aristarchus CF values to a FeO abundance of 19.3 +/− 2.2 wt. % (Table 3). This value is within one standard deviation of the FeO abundance calculated by *Wilcox et al.* [2006]. These estimates of FeO abundance indicate that the Aristarchus LPD lies near the middle of the compositional range of lunar pyroclastic glasses [*Delano*, 1986], and is somewhat less FeO-rich than the pyroclastic glass understood to represent the Taurus Littrow deposit, with an FeO abundance of 22.7 wt. %.

[29] *Sulpicius Gallus.* This large LPD, covering an area of 4,322 km^2 [*Gaddis et al.*, 2003], spans the mare/highland boundary on the western edge of Mare Serenitatis. The deposit contains local concentrations of red and orange material thought to be pyroclastic glass [*Weitz et al.*, 1999]. Parts of the Sulpicius Gallus LPD have a higher albedo than the Taurus Littrow LPD, suggesting differing average compositions, possibly due to contamination by highland soil [*Lucchitta and Schmitt*, 1974; *Weitz et al.*, 1998]. *Wilcox et al.* [2006], using radiative transfer modeling, estimated that the Sulpicius Gallus LPD contains 17.25 wt. % FeO.

[30] Diviner CF values were averaged over a 2 × 2 km area near 20°9′N, 10°17′E (Figure 10). These data yield a mean CF value of 8.37 μm, with a standard deviation of 0.04 μm. Using the regression line in Figure 8, these values yield a calculated FeO concentration of 21.6 +/− 3.0 wt. % (Table 3). This value is significantly higher than the FeO abundance calculated by *Wilcox et al.* [2006]. The difference may reflect localized mixing of underlying highland material with the pyroclastic glass, which would lower the FeO abundance of the mixture below that of pure glass, in the location measured by *Wilcox et al.* [2006].

[31] *Rima Fresnel.* This LPD, centered on a set of subparallel fissures, mantles highlands material near a mare/highland boundary and covers approximately 307 km^2 [*Gaddis et al.*, 2003]. *Blewett and Hawke* [2001] used maps based on Clementine multispectral data to estimate a FeO abundance of 15.1 +/− 0.4 wt. %. This value is close to that of typical Apollo 15 mare soils, as well as to that of Apollo 15 green glass (Table 1). *Blewett and Hawke* [2001] concluded, based on near-infrared telescopic spectra, that the Rima Fresnel deposit is dominated by mare basalt fragments rather than pyroclastic glass.

[32] The mean Diviner CF values for a pair of closely spaced 2 × 2 km areas centered near 28°3′N, 4°18′E are 8.32 +/− 0.04 μm and 8.29 μm +/− 0.03 μm (Figure 11). Inserting these values into the regression line formula shown in Figure 8 yields FeO concentrations of 17.8 +/− 3.0 and

15.6 +/− 2.2 wt. % (Table 3). The two values, from areas only a few kilometers apart, illustrate the scale of heterogeneity of this deposit. These values are within one standard deviation of the FeO abundance estimated by *Blewett and Hawke* [2001]. Both values are considerably lower than the FeO abundances of most lunar pyroclastic glasses, and support the contention of *Blewett and Hawke* [2001] that the majority of material erupted at Rima Fresnel has a composition close to that of mare basalt.

5. Discussion

[33] *Laboratory and Orbital CF Values.* Comparison of Tables 1 and 2 demonstrates a systematic decrease between CF values derived from RELAB reflectance measurements of lunar soils plus pyroclastic glasses under ambient conditions and Diviner measurements of CF derived from the Apollo landing sites plus the Taurus Littrow LPD. The regression lines for RELAB and Diviner CF values correlated to FeO abundances from the same set of Apollo soils and glasses (Figures 4 and 8, respectively) have similarly high goodness of fit (r^2) values, indicating close correlations between CF and FeO in both cases. However, the slopes are significantly different: 35.48 for the RELAB regression and 74.24 for the Diviner regression.

[34] The differences are likely attributable to the thermal gradient in the upper several hundred micrometers of soil on the lunar surface, which is known to affect thermal infrared emission spectra [*Donaldson Hanna et al.*, 2012]. These authors measured the spectra of pure minerals in a simulated lunar environment, which mimics the lunar thermal gradient, and found that this effect shifts the CF wavelength to lower values and increases the overall spectral contrast. These shifts are in qualitative agreement with the differences between the RELAB and Diviner measurements reported in the present study. Experiments are underway to measure the thermal infrared spectra of lunar soil samples in a simulated lunar environment [*Thomas et al.*, 2012], which should provide a more realistic comparison to the Diviner measurements.

[35] *Effects of TiO_2.* The colors of lunar pyroclastic glasses are closely correlated to their compositions, most directly to the abundance of titanium. This is clearly demonstrated in the descriptions and compositions of 25 distinct pyroclastic glasses [*Delano*, 1986], which show a systematic color shift from green thru yellow, orange, and red with increasing titanium content. Visible color in this sample set is much less strongly correlated to FeO abundance.

[36] The correlation changes, however, in the thermal infrared. Spectra in the 8 μm region, discussed in this paper, are sensitive to the iron abundances in mafic silicates but are relatively insensitive to iron or other cations in oxides. The major titanium-bearing phase in lunar soil and pyroclastic glass is ilmenite. The CF wavelength for ilmenite is near 12 μm, and the spectrum is essentially flat in the vicinity of 8 μm [*Logan et al.*, 1973]. Thus, a significant shift attributable to ilmenite in the CF values for lunar soil or pyroclastic glass is not anticipated.

[37] As discussed above, the correlation between CF measured by RELAB and titanium abundance (reported as TiO_2) shows a considerable degree of scatter (Figure 5). The goodness of fit (r^2) value is 0.58 and the low-titanium green glass sample falls well off the regression line. In contrast, the correlation between CF and FeO abundance for the same sample set (Figure 4) is stronger (r^2 = 0.83), and both pyroclastic glass samples fall close to the regression line. A similar close correlation exists between Diviner CF values and sample FeO concentrations (Figure 8). Thus, CF is a stronger predictor for the lunar soil and glass concentration of iron than that of titanium.

[38] *Effects of Crystallinity.* Lunar pyroclastic deposits consist of a mixture of glass beads and their crystallized isochemical equivalents. This is clearly evident in the Apollo 17 "orange soil" samples, which contain different mixtures of orange glass beads and black, crystallized beads dominated by ilmenite (Figure 2). Variations in visible and near-infrared spectral signatures across lunar pyroclastic deposits have been attributed to variations in the degree of crystallinity [*Lucey et al.*, 1998; *Pieters et al.*, 1974].

[39] Thermal infrared spectral features, however, appear to be insensitive to variations in crystallinity. Laboratory reflectance measurements of crystalline and glassy terrestrial plagioclase feldspars showed no change in CF with a phase change from crystalline to glass [*Nash and Salisbury*, 1991].

[40] A further indication of the effects of crystallinity on thermal infrared spectra is provided by shock experiments. *Johnson et al.* [2002] exposed terrestrial anorthosite and orthopyroxenite (bronzite) to peak pressures of 17–63 GPa. The CF wavelengths in the powdered anorthosite spectra were consistently shifted to higher values with increasing shock pressure. However, the iron-rich orthopyroxenite spectra, including CF wavelengths, showed only small changes with no consistent shifts correlated to increasing shock pressure. To the extent that shock can change the crystallinity of glass and minerals, these results argue for a minimal effect of differing crystallinity on the CF values for iron-rich pyroclastic samples.

[41] Finally, as discussed above, RELAB spectra were obtained for five Apollo 17 drill core samples, dominated by pyroclastic glass with orange and black glass beads in ratios ranging from approximately 70:30 to 20:80 [*Nagle*, 1978]. The mean CF wavelength measured for these five samples was 8.63 μm, with a standard deviation of 0.02 μm. No systematic shift in CF wavelength with variations in crystallinity was apparent.

[42] *Effects of Soil Maturity.* Maturity, the duration of exposure to the space environment, changes the optical properties of soils on airless bodies in systematic ways that include spectral darkening, reddening, and subdued absorption bands [*Hapke*, 2001]. Increasing maturity also shifts the CF wavelength of lunar soils to higher values [*Greenhagen et al.*, 2010]. This effect is demonstrated in Figure 6, wherein mature soil near the Apollo 16 landing site has a CF value of 8.15 +/− 0.01 μm, while the CF values for relatively fresh crater ejecta ranges around 8.0 μm. In the current study only relatively mature soil samples (I_s/FeO > 50) were included, in order to minimize the shifts in CF values caused by differences in maturity.

[43] *Error Analysis.* Five lunar soil samples of similar maturity were selected from a consistently characterized set described by the LSCC. These soils represent five of the six Apollo landing sites, and span the range of soil compositions in the Apollo collection. The 20–45 μm sieve fraction chosen for each soil is the size range thought to have the greatest

influence on thermophysical properties. The two pyroclastic glass samples, similarly fine-grained, are the only such samples available in large enough volumes for RELAB analysis. The published FeO and TiO_2 abundances of the soils and glasses are considered precise to approximately 0.1 wt. % (absolute), and multiple analyses of Apollo 17 orange glass beads showed a variability of 0.2 wt. % (absolute). The reflectance minima (CF wavelengths) were derived from RELAB spectra with a spectral resolution of 0.01 μm.

[44] Diviner data were used to derive CF values for the lunar surface, with measurements taken near mid-day to minimize thermal effects and reducing those data using the most recent correction method. CF values were averaged over 2 $\times$ 2 km areas, which encompass approximately 80 Diviner "pixels." The standard deviations about these average values range from 0.01–0.04 μm, and reflect both the absolute precision of the Diviner CF derivations (<0.02 μm) and the physical variability of lunar soil and pyroclastic deposits at the scale of approximately 100 m. These standard deviation values, when translated into calculated FeO wt. %, provide the largest source of uncertainty in these abundances. The mean CF values for the five Apollo sites and the Taurus Littrow LPD are linearly correlated to sample FeO abundances, with a goodness of fit (r^2) value of 0.90. The mean CF value for each of the six sites fits the regression line within one standard deviation.

[45] The specific sites for analysis in the Aristarchus, Sulpicius Gallus, and Rima Fresnel pyroclastic deposits were chosen to represent minimally contaminated pyroclastic material, with CF values typical of each deposit and with low degrees of CF variation. The CF values were averaged over 2 $\times$ 2 km areas, and the standard deviations of the mean values ranged from 0.03 to 0.04 μm. These values yielded an uncertainty around each calculated FeO abundance of 4–6 wt. %.

[46] *Lunar Pyroclastic Deposits.* The FeO abundance of the Aristarchus LPD, calculated from orbital thermal infrared emissivity, is 19.3 +/− 2.2 wt. %. This value is close to a FeO abundance value of 20.75 wt. %, calculated from radiative transfer modeling. Ultraviolet and visible spectra indicate that the Aristarchus deposit is dominated by pyroclastic glass, and these FeO abundances are near the mid-range for glass beads found in lunar soil.

[47] The Diviner FeO abundance calculated for the Sulpicius Gallus LPD is 21.6 +/− 3.0 wt. %, near the high end of the range for pyroclastic glass beads. Calculations based on radiative transfer modeling yield a value of 17.25 wt. %, at the low end of the range for pyroclastic glass samples. The difference between the two calculations may be due to the varying degrees of contamination from highlands material at this site. Orbital spectroscopy indicates that this LPD is dominated by pyroclastic glass, and red and orange colors have been observed within the deposit. Red and orange glass beads in lunar soil are consistently iron-rich, with FeO abundances of 22–23 wt. %.

[48] The Rima Fresnel LPD has spectral characteristics consistent with basaltic fragments rather than glass beads. The FeO contents of two closely space areas, derived from Diviner CF values, are 17.8 +/− 3.0 and 15.6 +/− 2.2 wt. %. The FeO abundance derived from Clementine multispectral data is 15.1 +/− 0.4 wt. %. All of these values are at the low end, or outside the range, of FeO abundances in pyroclastic glass samples but typical of lunar mare basalts.

6. Conclusions

[49] The Diviner 8 μm-region channels were expressly chosen to allow estimation of the CF wavelengths corresponding to lunar soils. This study demonstrates the close correlation between Diviner CF values and lunar sample FeO abundances as well as the close correlation derived from laboratory CF measurements. The absolute CF values derived from laboratory measurements of lunar soils, however, are offset from Diviner values for the corresponding sampling sites. Additional research, including measuring lunar samples under a simulated lunar environment, is underway to fully characterize and reconcile these differences.

[50] The correlation of Diviner CF values to sample FeO abundances has provided interpretable estimates of FeO concentrations in the Aristarchus, Sulpicius Gallus, and Rima Fresnel pyroclastic deposits. The precision of the analyses is limited by the precision of the Diviner CF derivation, coupled with the inherent variability of the pyroclastic deposits. However, the FeO abundance derivations are precise enough to distinguish iron-rich from iron-poor pyroclastic glass deposits, as well as deposits formed by pyroclastic eruptions of basaltic fragments.

[51] Diviner measurements and the techniques developed in this initial study hold the potential to remotely determine FeO abundances in many lunar pyroclastic deposits. A better understanding of the compositions of these deposits will provide improved insight into the magmatic history and composition of the deep lunar interior, as well as an enhanced inventory of potential resources for future human exploration.

[52] **Acknowledgments.** We appreciate support from the Lunar Reconnaissance Orbiter Program, through the Diviner Lunar Radiometer Experiment (David Paige, Principal Investigator), for each of the authors. We thank Takahiro Hiroi and Carle Pieters for generously providing the RELAB spectral data and Larry Taylor for insight into the intricacies of lunar soil. Dorothy Oehler and Trent Hare improved our understanding of lunar orbital data sets. Thoughtful reviews by John Delano, Nicolle Zellner, and an anonymous reviewer considerably improved this manuscript.

References

Allen, C. C., R. V. Morris, and D. S. McKay (1996), Oxygen extraction from lunar soils and pyroclastic glass, *J. Geophys. Res.*, *101*, 26,085–26,095, doi:10.1029/96JE02726.

Blewett, D. T., and B. R. Hawke (2001), Remote sensing and geologic studies of the Hadley-Appenine region of the Moon, *Meteorit. Planet. Sci.*, *36*, 701–730, doi:10.1111/j.1945-5100.2001.tb01909.x.

Blewett, D. T., P. G. Lucey, and B. R. Hawke (1997), Clementine images of the lunar sample return stations: Refinement of FeO and TiO_2 mapping techniques, *J. Geophys. Res.*, *102*, 16,319–16,325, doi:10.1029/97JE01505.

Coombs, C. R., B. R. Hawke, and C. C. Allen (1998), Aristarchus plateau: As a potential lunar base site, in *Space 98*, edited by R. G. Galloway and S. Lokaj, pp. 608–615, Am. Soc. of Civ. Eng., New York.

Delano, J. (1986), Pristine lunar glasses: Criteria, data, and implications, *Proc. Lunar Planet. Sci. Conf.*, *16*th, 201–213.

Donaldson Hanna, K. L., M. B. Wyatt, I. R. Thomas, N. E. Bowles, B. T. Greenhagen, A. Maturilli, J. Helbert, and D. A. Paige (2012), Thermal infrared emissivity measurements under a simulated lunar environment: Application to the Diviner Lunar Radiometer Experiment, *J. Geophys. Res.*, *117*, E00H05, doi:10.1029/2011JE003862.

Gaddis, L. R., M. I. Staid, J. A. Tyburczy, B. R. Hawke, and N. E. Petro (2003), Compositional analyses of lunar pyroclastic deposits, *Icarus*, *161*, 262–280, doi:10.1016/S0019-1035(02)00036-2.

Graf, J. (1993), Lunar soils grain size catalog, *NASA Ref. Publ.*, *1265*, 466 pp.

Green, D. H., A. E. Ringwood, W. O. Hibberson, and N. G. Ware (1975), Experimental petrology of Apollo 17 mare basalts, *Proc. Lunar Planet. Sci. Conf.*, *6*th, 1975.

Greenhagen, B. T., et al. (2010), Global silicate mineralogy of the Moon from the Diviner Lunar Radiometer, *Science*, *329*, 1507–1509.

Greenhagen, B. T., P. G. Lucey, J. L. Bandfield, P. O. Hayne, J. P. Williams, and D. A. Paige (2011), The Diviner Lunar Radiometer compositional data products: Description and examples, *Lunar Planet. Sci.*, *XLII*, Abstract 2679.

Hapke, B. (2001), Space weathering from Mercury to the asteroid belt, *J. Geophys. Res.*, *106*, 10,039–10,073, doi:10.1029/2000JE001338.

Hawke, B. R., C. R. Coombs, L. R. Gaddis, P. G. Lucey, and P. E. Owensby (1989), Remote sensing and geologic studies of localized dark mantle deposits on the Moon, *Proc. Lunar Planet. Sci. Conf.*, *19*th, 255–268.

Head, J. W., III (1974), Lunar dark-mantle deposits: Possible clues to the distribution of early mare deposits, *Proc. Lunar Planet. Sci. Conf.*, *5*th, 207–222.

Heiken, G. H., D. S. McKay, and R. W. Brown (1974), Lunar deposits of possible pyroclastic origin, *Geochim. Cosmochim. Acta*, *38*, 1703–1718, doi:10.1016/0016-7037(74)90187-2.

Johnson, J. R., F. Horz, P. G. Lucey, and P. R. Christensen (2002), Thermal infrared spectroscopy of experimentally shocked anorthosite and pyroxenite: Implications for remote sensing of Mars, *J. Geophys. Res.*, *107*(E10), 5073, doi:10.1029/2001JE001517.

Korotev, R. L. (1987), Mixing levels, the Apennine Front soil component, and compositional trends in the Apollo 15 soils, *Proc. Lunar Planet. Sci. Conf.*, *17*th, 411–431.

Lawrence, D. J., W. C. Feldman, R. C. Elphic, R. C. Little, T. H. Prettyman, S. Maurice, P. G. Lucey, and A. B. Binder (2002), Iron abundances on the lunar surface as measured by the Lunar Prospector gamma-ray and neutron spectrometers, *J. Geophys. Res.*, *107*(E12), 5130, doi:10.1029/2001JE001530.

Le Mouélic, S., P. G. Lucey, Y. Langevin, and B. R. Hawke (2002), Calculating iron contents of lunar highland materials surrounding Tycho crater from integrated Clementine UV-visible and near-infrared data, *J. Geophys. Res.*, *107*(E10), 5074, doi:10.1029/2000JE001484.

Logan, L. M., G. R. Hunt, J. W. Salisbury, and S. R. Balsamo (1973), Compositional implications of Christiansen frequency maximums for infrared remote sensing applications, *J. Geophys. Res.*, *78*, 4983–5003, doi:10.1029/JB078i023p04983.

Logan, L. M., G. R. Hunt, and J. W. Salisbury (1975), The use of mid-infrared spectroscopy in remote sensing of space targets, in *Infrared and Raman Spectroscopy of Lunar and Terrestrial Minerals*, edited by C. Karr, pp. 117–142, Academic, San Diego, Calif.

Lucchitta, B. K., and H. H. Schmitt (1974), Orange material in the Sulpicius Gallus formation at the southwestern edge of Mare Serenitatis, *Proc. Lunar Planet. Sci. Conf.*, *5*th, 223–234.

Lucey, P. G., G. J. Taylor, and E. Malaret (1995), Abundance and distribution of iron on the Moon, *Science*, *268*, 1150–1153, doi:10.1126/science.268.5214.1150.

Lucey, P. G., D. T. Blewett, and B. R. Hawke (1998), Mapping the FeO and TiO_2 content of the lunar surface with multispectral imagery, *J. Geophys. Res.*, *103*, 3679–3699, doi:10.1029/97JE03019.

Lucey, P. G., D. T. Blewett, and B. L. Jolliff (2000), Lunar iron and titanium abundance algorithms based on final processing of Clementine ultraviolet-visible images, *J. Geophys. Res.*, *105*, 20,297–20,305, doi:10.1029/1999JE001117.

McKay, D. S., G. H. Heiken, and G. Waits (1978), Core 74001/2: Grain size and petrology as a key to the rate of in-situ reworking and lateral transport on the lunar surface, *Proc. Lunar Planet. Sci. Conf.*, *9*th, 1913–1932.

Morris, R. V. (1978), The surface exposure/maturity of lunar soils–some concepts and I_s/FeO compilation, *Proc. Lunar Planet. Sci. Conf.*, *9*th, 2287–2297.

Nagle J. S. (1978), A comparison of a lunar and a terrestrial volcanic section, *Proc. Lunar Planet. Sci. Conf.*, *9*th, 1509–1526.

Nash, D. B. (1991), Infrared reflectance spectra (4 to 12 microns) of typical lunar samples, *Geophys. Res. Lett.*, *18*, 2145–2147, doi:10.1029/91GL02623.

Nash, D. B., and J. W. Salisbury (1991), Infrared reflectance spectra (2.2–15 μm) of plagioclase feldspars, *Geophys. Res. Lett.*, *18*, 1151–1154, doi:10.1029/91GL01008.

Paige, D. A., et al. (2009), The Lunar Reconnaissance Orbiter Diviner Lunar Radiometer Experiment, *Space Sci. Rev.*, *150*, 125–160, doi:10.1007/s11214-009-9529-2.

Pieters, C. M., and T. Hiroi (2004), RELAB (Reflectance Experiment Laboratory): A NASA multiuser spectroscopy facility, *Lunar Planet Sci.*, *IIIV*, Abstract 1720.

Pieters, C. M., T. B. McCord, M. P. Charett, and J. B. Adams (1974), Lunar surface: Identification of the dark mantling material in the Apollo 17 soil samples, *Science*, *183*, 1191–1194, doi:10.1126/science.183.4130.1191.

Pieters, C. M., E. M. Fischer, O. Rode, and A. Basu (1993), Optical effects of space weathering: The role of the finest fraction, *J. Geophys. Res.*, *98*, 20,817–20,824, doi:10.1029/93JE02467.

Saal, A. E., E. H. Hauri, M. L. Cascio, J. A. Van Orman, M. C. Rutherford, and R. F. Cooper (2008), Volatile content of lunar volcanic glasses and the presence of water in the Moon's interior, *Nature*, *454*, 192–195, doi:10.1038/nature07047.

Salisbury, J. W., G. R. Hunt, and L. M. Logan (1973), Infrared spectra of Apollo 16 fines, *Proc. Lunar Planet. Sci. Conf.*, *4*th, 3191–3196.

Taylor, L. A., C. M. Pieters, L. P. Keller, R. V. Morris, and D. S. McKay (2001), Lunar mare soils: Space weathering and the major effects of surface-correlated nanophase Fe, *J. Geophys. Res.*, *106*, 27,985–27,999, doi:10.1029/2000JE001402.

Taylor, L. A., C. Pieters, A. Patchen, D.-H. S. Taylor, R. V. Morris, L. P. Keller, and D. S. McKay (2010), Mineralogical and chemical characterization of lunar highland soils: Insights into the space weathering of soils on airless bodies, *J. Geophys. Res.*, *115*, E02002, doi:10.1029/2009JE003427.

Thomas, I. R., N. E. Bowles, T. Warren, B. T. Greenhagen, K. E. Donaldson-Hanna, and D. A. Paige (2012), Thermal infrared emission and goniometric laboratory measurements, *Lunar Planet. Sci.*, *XVIII*, Abstract 2637.

Weitz, C. M., J. W. Head III, and C. M. Pieters (1998), Lunar regional dark mantle deposits: Geologic, multispectral, and modeling studies, *J. Geophys. Res.*, *103*, 22,725–22,759, doi:10.1029/98JE02027.

Weitz, C. M., M. J. Rutherford, J. W. Head III, and D. S. McKay (1999), Ascent and eruption of a lunar high-titanium magma as inferred from the petrology of the 74001/2 drill core, *Meteorit. Planet. Sci.*, *34*, 527–540, doi:10.1111/j.1945-5100.1999.tb01361.x.

Wilcox, B. B., P. G. Lucey, and J. J. Gillis (2005), Mapping iron in the lunar mare: An improved approach, *J. Geophys. Res.*, *110*, E11001, doi:10.1029/2005JE002512.

Wilcox, B. B., P. G. Lucey, and B. R. Hawke (2006), Radiative transfer modeling of compositions of lunar pyroclastic deposits, *J. Geophys. Res.*, *111*, E09001, doi:10.1029/2006JE002686.